



1    **Soil trace gas fluxes along orthogonal precipitation and soil fertility gradients in tropical**  
2    **lowland forests of Panama**

3

4    Amanda L. Matson<sup>\*1</sup>, Marife D. Corre<sup>\*1</sup>, Kerstin Langs<sup>1</sup> and Edzo Veldkamp<sup>1</sup>

5    <sup>\*</sup>These authors contributed equally to this work

6

7    <sup>1</sup>Buesgen Institute, Soil Science of Tropical and Subtropical Ecosystems, Georg-August  
8    University, Buesgenweg 2, 37077, Goettingen, Germany

9

10

11    *Correspondence to:* Amanda L. Matson (amatson@gwdg.de)



## 12 Abstract

13 Tropical lowland forest soils are significant sources and sinks of trace gases. In order to model  
14 soil trace gas flux for future climate scenarios, it is necessary to be able to predict changes in soil  
15 trace gas fluxes along natural gradients of soil fertility and climatic characteristics. We quantified  
16 trace gas fluxes in lowland forest soils at five locations in Panama, which encompassed  
17 orthogonal precipitation and soil fertility gradients. Soil trace gas fluxes were measured monthly  
18 for one (NO) or two (CO<sub>2</sub>, CH<sub>4</sub>, N<sub>2</sub>O) years (2010-2012), using vented dynamic (for NO only) or  
19 static chambers with permanent bases. Across the five sites, annual fluxes ranged from: 8.0 to  
20 10.2 Mg CO<sub>2</sub>-C ha<sup>-1</sup> yr<sup>-1</sup>, -2.0 to -0.3 kg CH<sub>4</sub>-C ha<sup>-1</sup> yr<sup>-1</sup>, 0.4 to 1.3 kg N<sub>2</sub>O-N ha<sup>-1</sup> yr<sup>-1</sup> and -0.82  
21 to -0.03 kg NO-N ha<sup>-1</sup> yr<sup>-1</sup>. Soil CO<sub>2</sub> emissions did not differ across sites, but did exhibit clear  
22 seasonal differences and a parabolic pattern with soil moisture across sites. All sites were CH<sub>4</sub>  
23 sinks; within-site fluxes were largely controlled by soil moisture whereas fluxes across sites were  
24 positively correlated with an integrated index of soil fertility. Soil N<sub>2</sub>O fluxes were low  
25 throughout the measurement years, but highest emissions occurred at a mid-precipitation site  
26 with high soil N availability. NO uptake in the soil occurred at all sites, with the highest uptake  
27 at the low-precipitation site closest to Panama City; NO uptake was likely due to high ambient  
28 NO concentrations from anthropogenic sources. Our study highlights the dual importance of  
29 short-term (climatic) and long-term (soil/site characteristics) factors in predicting soil trace gas  
30 fluxes.

31

32 *Keywords:* greenhouse gases, carbon dioxide, methane, nitric oxide, nitrous oxide, tropical forest



## 33 **1 Introduction**

34 Soils can be both sources and sinks of carbon dioxide (CO<sub>2</sub>), methane (CH<sub>4</sub>), nitrous oxide  
35 (N<sub>2</sub>O) and nitric oxide (NO). Tropical forest soils, specifically, are the largest natural source of  
36 soil CO<sub>2</sub> (Raich and Schlesinger, 1992) and N<sub>2</sub>O (Bouwman et al., 1993; Prather et al., 1995)  
37 and can be significant sinks of CH<sub>4</sub> (Steudler et al., 1996; Keller et al., 2005; Sousa Neto et al.,  
38 2011). Although soil NO fluxes in tropical forests are often low (Keller and Reiners, 1994;  
39 Koehler et al., 2009b), and the canopy can act as a sink for a large proportion of soil-emitted NO  
40 (Rummel et al., 2002), even low emissions may be important in regulating atmospheric oxidant  
41 production (Keller et al., 1991; Chameides et al., 1992). Studies from Central and South  
42 American (CSA) tropical lowland forests have measured a large range of annual soil trace gas  
43 fluxes; in one case, N<sub>2</sub>O emissions varied by one order of magnitude within a single study (1.23  
44 to 11.39 kg N ha<sup>-1</sup> yr<sup>-1</sup>; Silver et al., 2005). Such disparity in measurements, caused by the  
45 temporal and spatial variability found in tropical forests (Townsend et al., 2008), makes it  
46 challenging to model soil trace gas fluxes from these areas and to predict how they might be  
47 affected by climate change.

48 Temporal variations in soil trace gas fluxes are primarily correlated with temperature and  
49 moisture. Temperature is often more important where there are annual extremes in temperature -  
50 such as in temperate and boreal regions - whereas precipitation and soil moisture are more  
51 important in tropical regions, where air temperature does not vary much throughout the year  
52 (Saikawa et al., 2013). Soil temperature in CSA tropical forests can be positively correlated with  
53 soil CO<sub>2</sub> emissions (Chambers et al., 2004; Schwendenmann and Veldkamp, 2006; Sotta et al.,  
54 2006, Koehler et al., 2009a) and NO flux (Gut et al., 2002), and negatively correlated with soil  
55 N<sub>2</sub>O emissions (Keller et al., 2005), though the latter may be due to a co-correlation of soil



56 temperature with soil moisture (see below). For soil CH<sub>4</sub> fluxes, given that the activity of both  
 57 methanotrophs (CH<sub>4</sub> consumers) and methanogens (CH<sub>4</sub> producers) can increase with  
 58 temperature (Conrad, 1996; Chin et al., 1999; Mohanty et al., 2007), net changes of soil CH<sub>4</sub>  
 59 fluxes in response to temperature may be driven by other site conditions, such as soil moisture.

60 Soil moisture affects microbial activity, which leads to trace gas production or  
 61 consumption, both directly through water availability and indirectly through its influence on the  
 62 soil oxygen status and gas diffusivity (Davidson and Schimel, 1995). Soil CO<sub>2</sub> emissions from  
 63 CSA tropical forest soils generally exhibit positive relationships with soil moisture (Davidson et  
 64 al., 2000), which may be parabolic, with emissions increasing until the threshold at which  
 65 anaerobic conditions start to inhibit soil CO<sub>2</sub> production and/or gas diffusion and then decreasing  
 66 (Schwendenmann et al., 2003; Sotta et al., 2006; Kohler et al., 2009a). Soil CH<sub>4</sub> fluxes (positive  
 67 values for net emissions and negative values for net consumption) in CSA tropical lowland  
 68 forests also tend to exhibit positive correlations with soil moisture (Keller and Reiners, 1994;  
 69 Verchot et al., 2000; Davidson et al., 2004; Veldkamp et al., 2013) since high soil moisture  
 70 conditions favor CH<sub>4</sub> production, while CH<sub>4</sub> consumption is reduced due to inhibited diffusion of  
 71 CH<sub>4</sub> from the atmosphere to the soil (Le Mer and Roger, 2001; Koehler et al., 2012; Veldkamp et  
 72 al., 2013). In general, soil NO production through nitrification dominates in aerobic conditions  
 73 whereas soil N<sub>2</sub>O production through denitrification dominates in anaerobic conditions (Conrad,  
 74 2002). Therefore, as shown in several CSA tropical forest studies (Keller and Reiners, 1994;  
 75 Verchot et al., 1999; Davidson et al., 2004; Keller et al., 2005; Koehler et al., 2009b), with  
 76 increases in soil moisture, soil NO fluxes generally decrease (though Gut et al., 2002 show that  
 77 this relationship is complex) while soil N<sub>2</sub>O fluxes increase.



78           Spatial variations in soil trace gas fluxes are largely controlled by soil physical and  
79   biochemical characteristics. Soil texture strongly influences soil water retention and gas  
80   diffusivity (Koehler et al. 2010; Hassler et al. 2015) as well as soil fertility, plant productivity,  
81   decomposition and ultimately soil N availability (Silver et al., 2000; Sotta et al., 2008; Allen et  
82   al., 2015). In CSA tropical forests, both Silver et al. (2005) and Sotta et al. (2006) observed  
83   higher soil CO<sub>2</sub> emissions from sandy than clayey Ferralsol soils, which were attributed to  
84   respiration from the higher fine root biomass in the sandy soils. Soil N-oxide fluxes may also be  
85   affected by soil texture; soil N<sub>2</sub>O emissions can be stimulated by the higher soil N availability  
86   and greater proportion of anaerobic microsites in clayey soils (Keller et al., 2005; Silver et al.,  
87   2005; Sotta et al., 2008) whereas soil NO fluxes can be facilitated by the higher diffusivity in  
88   sandy soils (Silver et al., 2005). Although they have less often been the focus of trace gas  
89   studies, soil biochemical characteristics (i.e. soil fertility status) also play an important role in  
90   soil trace gas fluxes. Schwendenmann et al. (2003) observed a positive relationship between soil  
91   CO<sub>2</sub> flux and spatial differences in soil organic C and total N, and a negative relationship with  
92   soil total P (possibly due to lower fine root biomass in areas of high P). Veldkamp et al. (2013)  
93   reported that increases in soil N availability stimulate CH<sub>4</sub> uptake and/or reduce CH<sub>4</sub> production  
94   in soil, and Hassler et al. (2015) also showed that soil fertility (i.e. increased soil N availability  
95   and decreased soil exchangeable Al) enhances soil CH<sub>4</sub> uptake. Finally, as an essential substrate  
96   for nitrification and denitrification, N availability in the soil is the primary controlling factor of  
97   soil N-oxide fluxes (Koehler et al., 2009b; Corre et al., 2014).

98           Climate scenarios suggest that tropical regions may experience large changes in  
99   precipitation regimes in the future, with moist tropical regions likely experiencing both higher  
100   annual precipitation and more extreme precipitation events (Stocker et al., 2013). Such changes



could significantly alter current soil trace gas fluxes, since soil moisture – as described above – plays an important role in both the temporal and spatial variability of soil trace gas fluxes. One approach to studying how changes in precipitation may alter soil trace gas fluxes is to investigate these fluxes along a natural gradient of climate (e.g. precipitation) in a localized region. This approach was used by Holtgrieve et al. (2006) on the Kula volcanic series lava flow in Hawaii, to show that soil N cycling and N-oxide fluxes were strongly affected by mean annual precipitation. However, as suggested by Santiago et al. (2005), precipitation gradients in continental tropical forests, where there are variations in species composition and soil parent material, may exhibit different patterns than those from Hawaii. Additionally, precipitation (or climate) is itself a soil forming factor (Jenny, 1945), and continental tropical lowland soils are considerably older than the relatively young volcanic soils (i.e. Santiago et al., 2005). Therefore, soils of continental precipitation gradients will reflect both the long-term effects of the precipitation regime (i.e. on differences in soil physical and biochemical characteristics) in addition to short-term effects (i.e. on soil moisture).

In this study, we quantified soil trace gas fluxes in tropical lowland forests of the Panama Canal Watershed, spanning a precipitation gradient of 1700–3400 mm yr<sup>-1</sup> (Figure S1). Soil fertility (based on an aggregate index that included clay content, <sup>15</sup>N natural abundance, effective cation exchange capacity (ECEC), organic C:N ratio, and exchangeable Al; see 2.4) varied orthogonally with this precipitation gradient (Figure S2). The objectives of our study were to: (1) determine how soil fluxes of CO<sub>2</sub>, CH<sub>4</sub>, N<sub>2</sub>O and NO vary along orthogonal gradients of precipitation and soil fertility, and (2) assess and compare the spatial and temporal controls of soil trace gas fluxes in lowland tropical forests. By using orthogonal gradients of precipitation and soil fertility, we were able to examine the relative importance of climatic factors vs. soil



124 biochemical characteristics for soil trace gas fluxes. We hypothesized that the temporal and  
 125 spatial patterns of soil trace gas fluxes across sites would follow the pattern of the most  
 126 important controlling soil factors: soil CO<sub>2</sub> fluxes would be parabolic in relation to increasing  
 127 soil moisture along the precipitation gradient; soil CH<sub>4</sub> fluxes would increase (or CH<sub>4</sub>  
 128 consumption would decrease) with increasing soil moisture and decreasing soil fertility along the  
 129 precipitation gradient; and soil NO fluxes would decrease whereas soil N<sub>2</sub>O fluxes would  
 130 increase with increasing soil moisture along the precipitation gradient.

131

## 132 **2 Methods**

### 133 **2.1 Study sites**

134 Soil trace gas fluxes were measured in five study sites of the Center for Tropical Forest Science  
 135 (CTFS) located in the Panama Canal Watershed, central Panama (Table 1; Figure S1). Mean  
 136 annual air temperature is 27 °C (Windsor, 1990); the soil temperature across all sites fluctuated  
 137 between 22.5 and 27.5 °C during our study years (Fig. 1a). The five sites span a gradient of  
 138 annual precipitation from 1700 mm yr<sup>-1</sup> in Metropolitan National Park (Met) on the Pacific side  
 139 to 3400 mm yr<sup>-1</sup> in P32 on the Atlantic side; the dry season generally lasts from January through  
 140 April (Corre et al., 2014). The sites were located in either old growth (P8 and P32) or mature  
 141 secondary (Met, P27, and P19) lowland forests, with tree densities ( $\geq 10$  cm diameter at breast  
 142 height, DBH) of: 322 stems ha<sup>-1</sup> in Met, 395 stems ha<sup>-1</sup> in P27, 560 stems ha<sup>-1</sup> in P8, 520 stems  
 143 ha<sup>-1</sup> in P19, and 537 stems ha<sup>-1</sup> in P32 (Pyke et al., 2001). Since precipitation and parent  
 144 materials vary across these sites, soil types also vary from Cambisols (Met and P27) on the  
 145 Pacific side to Ferralsols (P8, P19, and P32) on the Atlantic side (Table 1). Floristic composition  
 146 in these sites has been shown to be correlated with both regional precipitation and geology/soil



147 attributes (Pyke et al., 2001). The amounts and forms of soil organic P are strongly controlled by  
148 soil properties whereas the proportion of soil organic P to total P is insensitive to the variation in  
149 rainfall and soil properties (Turner and Engelbrecht, 2011).

150

## 151 **2.2 Soil trace gas flux measurement**

152 Soil CO<sub>2</sub>, CH<sub>4</sub> and N<sub>2</sub>O fluxes were measured every 2-4 weeks from June 2010 through  
153 February 2012 (28-31 sampling dates) using static vented chambers. Within each of the five  
154 sites, a 20 m grid was placed over a 1 ha area and we randomly chose four 20 m x 20 m replicate  
155 plots with a minimum distance of 20 m between plots. In each replicate plot, four permanent  
156 chamber bases were installed (0.04 m<sup>2</sup> area and 0.25 m height after inserting 2 cm into the soil)  
157 at the ends of two perpendicular 20 m transects that crossed in the plot's center. The total volume  
158 of the chamber (with cover) was 11 L. To measure soil trace gas fluxes, chamber covers were  
159 placed on the bases and gas samples (100 mL) were taken 2, 12, 22 and 32 min later. Samples  
160 were stored in pre-evacuated glass containers with Teflon-coated stopcocks. At the Gamboa field  
161 laboratory, gas samples were then analyzed for CO<sub>2</sub>, CH<sub>4</sub> and N<sub>2</sub>O concentrations using a gas  
162 chromatograph (Shimadzu GC-14B, Columbia, MD, USA) equipped with a flame ionization  
163 detector (FID), an electron capture detector (ECD) and an autosampler, the same instrument that  
164 was used in our earlier studies (Koehler et al. 2009a, 2009b, 2010, 2012; Veldkamp et al., 2013;  
165 Corre et al. 2014). Gas concentrations were determined by comparing integration peaks with  
166 those of three or four standard gases containing increasing concentrations of CO<sub>2</sub>, CH<sub>4</sub> and N<sub>2</sub>O  
167 (Deuste Steininger GmbH, Mühlhausen, Germany).

168 Soil NO fluxes were measured every 2-4 weeks from June 2010 through June 2011 (18-  
169 21 sampling dates) using open dynamic chambers (11 L volume) placed for 5-7 minutes on the





170 same permanent bases described above. The air from the chamber was sampled by a pump with a  
171 flow rate of  $0.5\text{--}0.6\text{ L min}^{-1}$ , passed through a  $\text{CrO}_3$  catalyst that oxidizes NO to  $\text{NO}_2$ , and flowed  
172 across a fabric wick that is saturated with a luminol solution. The luminol then oxidizes and  
173 produces chemiluminescence, which is proportional to the concentration of  $\text{NO}_2$ , and is  
174 measured with a Scintrex LMA-3 chemiluminescence detector (ScintrexUnisearch, Ontario,  
175 Canada). To minimize deposition losses within the sampling system, all parts in contact with the  
176 sample gas are made of Teflon (PTFE). To prevent contamination of tubing and analyzers,  
177 particulate matter is removed from the sampled air by PTFE particulate filters (pore size:  $5\text{ }\mu\text{m}$ ).  
178 In order to minimize potential changes in catalyst efficiency caused by variations of air humidity,  
179 a known flux of ambient air dried by silica gel was mixed to the sampled air to maintain a  
180 humidity of  $\sim 50\%$ ; the detector was also calibrated in-situ prior to and following chamber  
181 measurements, using a standard gas (3000 ppb NO; DeusteSteininger GmbH, Mühlhausen,  
182 Germany).

183 Soil trace gas fluxes were calculated as the linear change in concentration over time, and  
184 were adjusted for air temperature and atmospheric pressure measured during or directly after  
185 sampling; zero fluxes were included in the data statistical analysis. Annual soil NO fluxes were  
186 calculated using the June 2010–May 2011 measurements and annual soil  $\text{CO}_2$  and  $\text{N}_2\text{O}$  fluxes  
187 were calculated using the January to December 2011 measurements; annual fluxes were  
188 calculated using the trapezoid rule between days with measured fluxes (Koehler et al. 2009a,  
189 2009b, 2010; Veldkamp et al., 2013; Corre et al. 2014).

190



### 191    **2.3 Soil biochemical characteristics**

192    In each replicate plot after each soil trace gas flux measurement, samples of the top 5 cm of soil  
193    were taken about 1 m from each of the 4 chamber bases, pooled and mixed thoroughly in the  
194    field to measure soil extractable  $\text{NH}_4^+$  and  $\text{NO}_3^-$  concentrations and gravimetric water content. In  
195    the field, soil samples were placed into prepared extraction bottles containing 150 mL of 0.5M  
196     $\text{K}_2\text{SO}_4$  and shaken thoroughly. Back at the field station ( $\leq 6$  h after samples were taken), the  
197    extraction bottles were again shaken ( $\sim 1$  h) and then the extracts were filtered and frozen  
198    immediately. The remaining soil was oven-dried at 105 °C for 1 day in order to ascertain  
199    gravimetric water content; this was then used to calculate the dry mass of the soil that had been  
200    extracted for mineral N. The frozen extracts were sent by air to the University of Göttingen,  
201    Germany for analysis by continuous flow injection colorimetry (Cenco/Skalar Instruments,  
202    Breda, Netherlands). The Berthelot reaction method was used to determine  $\text{NH}_4^+$  (Skalar Method  
203    155-000) and the copper-cadmium reduction method was used to determine  $\text{NO}_3^-$  ( $\text{NH}_4\text{Cl}$  buffer  
204    without ethylenediaminetetraacetic acid; Skalar Method 461-000).

205        Soil pits were dug in the center of each of the four replicate plots per site and soil samples  
206    were taken for the depth intervals of 0-5, 5-10, 10-25 and 25-50 cm. Soil samples were air-dried  
207    and sieved through a 2-mm sieve. Natural abundance  $^{15}\text{N}$  signatures were determined from the  
208    ground soil samples using isotope ratio mass spectrometry (IRMS; Delta Plus, Finnigan MAT,  
209    Bremen, Germany). We calculated the  $\delta^{15}\text{N}$  enrichment factor ( $\epsilon$ ) using the Rayleigh equation  
210    (Mariotti et al., 1981):  $\epsilon = d_s - d_{so} / \ln f$ , where  $d_s$  is the  $\delta^{15}\text{N}$  natural abundance at different depths  
211    in the soil profile,  $d_{so}$  is the  $\delta^{15}\text{N}$  natural abundance of the reference depth (top 5 cm), and  $f$  is the  
212    fraction of total N remaining (i.e. the total N concentration at a given depth divided by the total  
213    N concentration in the top 5 cm). The  $\epsilon$  value was used as an integrative indicator of soil N



availability, as this correlates with internal soil-N cycling rates (Sotta et al., 2008; Baldos et al., 2015). Total organic C and N were measured from the ground soil samples by dry combustion using a CN analyzer (ElementarVario EL; Elementar Analysis Systems GmbH, Hanau, Germany). ECEC was determined from the sieved soil samples by percolating with unbuffered 1M NH<sub>4</sub>Cl and measuring the exchangeable element concentrations (Ca, Mg, K, Mn, Na, Fe and Al) in the percolates using an inductively coupled plasma-atomic emission spectrometer (ICP-AES; Spectroflame, Spectro Analytical Instruments, Kleve, Germany). Base saturation was calculated as the ratio of exchangeable base cations to the ECEC. Soil pH (H<sub>2</sub>O) was analyzed from a 1:4 soil-to-water ratio. Particle size distribution of the mineral soil was determined using the pipette method with pyrophosphate as a dispersing agent (König and Fortmann, 1996).

224

#### 2.4. Soil fertility index

The variation in soil types along our rainfall gradient (Table 1) was paralleled with variations in soil biochemical characteristics (Table 2; see 3.1). Thus, we developed a soil fertility index using principal component analysis (PCA), similar to the approach employed by Swaine (1996); for each site, the index was based on five soil physical and biochemical properties: 1) clay content, which reflects water- and nutrient-holding capacity, 2)  $\epsilon$  that signifies long-term soil N status, 3) ECEC and soil C:N ratio, which indicate bioavailability of rock-derived nutrients and soil organic matter, and 4) exchangeable Al, which implies soil chemical suitability. We used the depth-weighted average of these soil parameters (Table 2), measured at various depth intervals in the top 50 cm depth (except for  $\epsilon$  that is calculated for the whole depth; see above). The first component factor of this PCA analysis explained 42 % of the variation in these soil characteristics among sites (Figure S2) and the factor scores were used as the quantitative index



237 of soil fertility for each of the four replicate plots per site. This analysis showed that soil fertility  
 238 of the five lowland forests varied orthogonally with the precipitation gradient (Figure S2).

239

## 240 **2.4 Statistical analyses**

241 We note that our statistical tests are based on the four replicate plots in each of the five 1-ha  
 242 forest sites along these orthogonal gradients of precipitation and soil fertility, and that the sites  
 243 themselves were not replicated along the gradients. Consequently, our interpretations and  
 244 conclusions are limited only to these studied sites.

245 Soil trace gas fluxes (based on the average of the four chambers per replicate plot on each  
 246 sampling day) and the accompanying soil explanatory variables (soil temperature, gravimetric  
 247 moisture,  $\text{NH}_4^+$  concentration and  $\text{NO}_3^-$  concentration) were tested for normality using Shapiro-  
 248 Wilk's test; variables with non-normal distributions were square root or log transformed. We  
 249 then used linear mixed effects models (LMEs) to assess the differences in these repeatedly-  
 250 measured variables along the orthogonal precipitation and soil fertility gradients, with site and/or  
 251 season as the fixed effect(s) and sampling days and replicate plots as random effects. If the  
 252 Akaike information criterion showed an improvement in the LME models, we included a first-  
 253 order temporal autoregressive function to account for the decreasing correlation of measurements  
 254 with increasing time (Zuur et al., 2009) and/or a variance function (varIdent) to account for  
 255 heteroscedasticity of fixed-factor variances (Crawley, 2012). To assess the relationships between  
 256 soil trace gas fluxes and soil explanatory variables, we used the mean values of the four replicate  
 257 plots on each sampling date, and conducted Pearson correlation tests over the entire sampling  
 258 period across the five sites and for each site.



For the soil biochemical characteristics measured only once (Table 2), differences in depth-weighted values (for the top 50 cm) among sites were evaluated using one-way analysis of variance followed by a Tukey HSD test. Their relationships with soil trace gas fluxes across the five sites (using annual values and average seasonal values) were tested using Spearman rank correlations. In all statistical tests, differences among sites or between seasons and correlation coefficients were considered significant at  $P \leq 0.05$ . Data analyses were conducted using the R open source software (R Core Team, 2013).

### 3 Results

#### 3.1 Soil biochemical characteristics

The soil  $\delta^{15}\text{N}$  natural abundance signatures and  $\epsilon$ , which are proxies of the long-term soil N status (i.e. the higher the values, the higher the soil N availability), were lower at the low-rainfall sites (Met and P27) than at one of the mid-rainfall sites (P19) ( $P \leq 0.05$ ; Table 2). Soil organic C was lower at one of the lower-rainfall sites (P27) than at the high-rainfall site (P32) whereas the differences in total soil N among sites paralleled the increase in annual precipitation ( $P \leq 0.05$ ; Table 2). Soil pH, ECEC and exchangeable bases generally showed the opposite trend to that of total soil N – higher values at the low-rainfall sites (with less-weathered soils) than at the mid- and high-rainfall sites (with highly weathered soils) (all  $P \leq 0.05$ ; Tables 1 and 2). Soil exchangeable Al showed the converse pattern to that of exchangeable bases ( $P \leq 0.02$ ; Table 2).

Of the four soil controlling factors that were monitored over time (temperature, moisture, extractable  $\text{NH}_4^+$  and extractable  $\text{NO}_3^-$ ; Fig. 1a-d), only moisture and extractable  $\text{NO}_3^-$  differed strongly between seasons ( $P < 0.01$ ; Fig. 1b-c; Table 3); soil moisture contents were higher in the wet season than the dry season at all sites, while extractable soil  $\text{NO}_3^-$  concentrations were lower



in the wet season that the dry season at all sites but P19. Within each season, all four soil controlling factors differed along the precipitation gradient (all  $P < 0.01$  except  $P = 0.04$  for extractable  $\text{NH}_4^+$  in the wet season; Table 3). Soil temperatures in both seasons were lower at P32 (3400 mm) than at all other sites (not significant at P27 in the dry season), and also lower at P27 (2030 mm) than Met (1700 mm). Soil moisture contents, in contrast, were higher in both seasons at P32 than at the other four sites. Extractable soil  $\text{NO}_3^-$  concentrations in both seasons were higher at Met and P8 (2360 mm) than at P27, P19 (2690 mm) and P32, and in the wet season, also higher at Met than P8. Extractable soil  $\text{NH}_4^+$  concentrations were higher at P32 than Met in both seasons. Across sites, over the 21-month measurement period, soil moisture was inversely correlated with temperature ( $r = -0.28$ ,  $P < 0.01$ ,  $n = 145$ ) and extractable soil  $\text{NO}_3^-$  ( $r = -0.51$ ,  $P < 0.01$ ,  $n = 145$ ) and directly correlated with extractable soil  $\text{NH}_4^+$  ( $r = 0.46$ ,  $P < 0.01$ ,  $n = 145$ ).

294

### 3.2 $\text{CO}_2$ fluxes

Although soil  $\text{CO}_2$  emissions did not differ among the five sites over the 21-month measurement period ( $P = 0.40$ ; Fig. 2a; Table 3), emissions exhibited a parabolic relationship with soil moisture across sites (Fig. 3) and were higher in the wet season than the dry season at each site ( $P \leq 0.05$ ; Table 3). Over the 21-month sampling period, average daily soil  $\text{CO}_2$  emissions from the five sites were correlated with soil temperature ( $r = 0.46$ ,  $P < 0.01$ ,  $n = 145$ ), soil moisture ( $r = 0.35$ ,  $P < 0.01$ ,  $n = 145$ ; Fig. 3), extractable soil  $\text{NH}_4^+$  ( $r = 0.32$ ,  $P < 0.01$ ,  $n = 145$ ) and extractable soil  $\text{NO}_3^-$  ( $r = -0.21$ ,  $P = 0.01$ ,  $n = 145$ ). Within individual sites, average daily soil  $\text{CO}_2$  emissions also exhibited negative correlations with extractable soil  $\text{NO}_3^-$  at Met ( $r = -0.48$ ,  $P = 0.01$ ,  $n = 27$ ), P8 ( $r = -0.39$ ,  $P = 0.03$ ,  $n = 30$ ), and P32 ( $r = -0.54$ ,  $P < 0.01$ ,  $n = 30$ ).



Similar to the relationship observed for average daily fluxes (Fig. 3), the annual soil CO<sub>2</sub> emissions (Table 4) also exhibited a parabolic pattern across the five sites of the precipitation gradient: high at the mid-rainfall sites (P8 and P19) and low at both ends of the precipitation gradient (Met and P32). There were no significant correlations between soil CO<sub>2</sub> emissions (neither for annual CO<sub>2</sub> fluxes nor for wet- and dry-season averages) and the soil biochemical characteristics (Table 5; Table S1).

311

### 3.3 CH<sub>4</sub> fluxes

On average, despite occasional emissions in the wet season (Fig. 2b), the soils in the five sites acted as CH<sub>4</sub> sinks (Tables 3 and 4). Comparing between seasons, soil CH<sub>4</sub> uptake was higher in the dry season than the wet season at all sites ( $P \leq 0.05$ ; Table 3). Differences among sites were the same in both seasons; soil CH<sub>4</sub> uptake at P19 (2690 mm) was higher than at Met (1700 mm), P27 (2030 mm) and P32 (3400 mm), and higher at P8 (2360 mm) than at Met ( $P \leq 0.05$ ; Table 3). Over the 21-month sampling period, average daily soil CH<sub>4</sub> fluxes from the five sites were positively correlated (i.e. soil CH<sub>4</sub> uptake decreased) with soil moisture ( $r = 0.44$ ,  $P < 0.01$ ,  $n = 145$ ; Fig. 4a). Within individual sites, average daily soil CH<sub>4</sub> fluxes at P8 ( $r = -0.63$ ,  $P < 0.01$ ,  $n = 30$ ), P19 ( $r = -0.48$ ,  $P < 0.01$ ,  $n = 28$ ) and P32 ( $r = -0.48$ ,  $P < 0.01$ ,  $n = 30$ ) also exhibited negative correlations with extractable soil NO<sub>3</sub><sup>-</sup> (i.e. soil CH<sub>4</sub> uptake increased as extractable soil NO<sub>3</sub><sup>-</sup> increased).

The annual soil CH<sub>4</sub> fluxes (Table 4) were positively correlated (Spearman  $\rho = 0.84$ ,  $P < 0.01$ ,  $n = 20$ ; Fig. 4b) with the soil fertility index (Figure S2) and negatively correlated with annual precipitation ( $\rho = -0.63$ ,  $P < 0.01$ ,  $n = 20$ ; Fig. 4c). Of the soil biochemical properties measured once, annual soil CH<sub>4</sub> fluxes were negatively correlated with soil <sup>15</sup>N natural



abundance and exchangeable Al, and positively correlated with ECEC, base saturation and pH (Table 5). Average seasonal soil CH<sub>4</sub> fluxes exhibited similar correlations (Table S1); it is notable that when correlation analysis was separated by season, correlations with soil <sup>15</sup>N natural abundance were stronger in the dry season than the wet season.

### 3.4 N<sub>2</sub>O fluxes

Soil N<sub>2</sub>O fluxes differed among sites only in the wet season and not in the dry season (Table 3; Fig. 2c); soil N<sub>2</sub>O emissions in the wet season were higher at P8 (2360 mm) than all other sites ( $P < 0.01$ ). Within individual sites, soil N<sub>2</sub>O emissions were higher in the wet season than the dry season at P8 and P19 (2690 mm) ( $P < 0.01$ ; Table 3). These two sites were also the only two to exhibit correlations with soil controlling factors; soil N<sub>2</sub>O emissions increased with increases in soil moisture at P8 ( $r = 0.69$ ,  $P < 0.01$ ,  $n = 30$ ) and P19 ( $r = 0.60$ ,  $P < 0.01$ ,  $n = 28$ ), and decreased with increases in soil NO<sub>3</sub><sup>-</sup> concentration at P8 ( $r = -0.57$ ,  $P < 0.01$ ,  $n = 30$ ) and P19 ( $r = -0.38$ ,  $P = 0.05$ ,  $n = 28$ ). Annual soil N<sub>2</sub>O emissions (Table 4) were negatively correlated with clay content (Table 5). Seasonal average soil N<sub>2</sub>O emissions were positively correlated with soil <sup>15</sup>N natural abundance in the wet season but not in the dry season (Table S1).

### 3.5 NO fluxes

In all five sites, net uptake of NO was measured more often than net NO emissions from the soil (Fig. 2d) and NO uptake was consistently higher ( $P \leq 0.05$ ) in the wet than dry season, except at P19 (2690 mm) where there was no difference between seasons (Table 3). Wet-season soil NO uptake at Met (1700 mm) was larger than all other sites ( $P < 0.01$ ; Table 3), while in the dry season soil NO uptake at P19 was larger than at P8 (2360 mm) and P32 (3400 mm) ( $P < 0.01$ ;





Table 3). Over the 13-month measurement period, soil NO fluxes were negatively correlated (i.e. net NO uptake increased) with ambient NO concentration ( $r = -0.34$ ,  $P < 0.01$ ,  $n = 103$ ; Fig. 5). Within individual site, only soil NO fluxes at P8 showed a negative correlation with soil moisture ( $r = -0.67$ ,  $P < 0.01$ ;  $n = 21$ ) and positive correlation (i.e. net NO uptake decreased) with extractable soil  $\text{NO}_3^-$  ( $r = 0.65$ ,  $P < 0.01$ ;  $n = 21$ ). There were no correlations with average seasonal soil NO fluxes in the wet season, but in the dry season average seasonal soil NO fluxes were negatively correlated with clay content across sites (Table S1).

358

## 359 **4 Discussion**

### 360 **4.1 CO<sub>2</sub> fluxes**

Soil CO<sub>2</sub> emissions from CSA tropical lowland forests, including Brazil (Davidson et al., 2000, Chambers et al., 2004, Silver et al., 2005, Sotta et al., 2006), Puerto Rico (Raich and Schlesinger, 1992), Panama (Kursar 1989, Koehler et al., 2009a; Nottingham et al., 2010) and Costa Rica (Schwendenmann and Veldkamp, 2006), range from 10.8 Mg C ha<sup>-1</sup> yr<sup>-1</sup> (Silver et al., 2005) to 39.7 Mg C ha<sup>-1</sup> yr<sup>-1</sup> (Sotta et al., 2006). Our annual soil CO<sub>2</sub> emissions (Table 4) were on the lower end of this range. When compared with other studies in lowland forests of Panama, our values were also at the lower end of those reported for Barro Colorado Island (BCI) (estimated at 14.5 Mg C ha<sup>-1</sup> yr<sup>-1</sup> in 1986; Kursar 1989) and Gigante (ranging from 13.59 ± 1.34 to 17.12 ± 1.59 Mg C ha<sup>-1</sup> yr<sup>-1</sup> between 2006 and 2008; Koehler et al., 2009a), which can, in part, be attributed to inter-annual variation. Soil CO<sub>2</sub> fluxes at Gigante varied by more than 3 Mg C ha<sup>-1</sup> yr<sup>-1</sup> between 2006 and 2008 (Koehler et al., 2009a), and fine litterfall, one of the substrates of heterotrophic respiration, also varied by about 2 Mg ha<sup>-1</sup> yr<sup>-1</sup> from 1998 to 2008 (with annual averages of 7.7-9.7 Mg ha<sup>-1</sup> yr<sup>-1</sup>; Wright et al., 2011). Moreover, our values were comparable



374 with that of a mature secondary forest (P15 site, 7–18 Mg C ha<sup>-1</sup> yr<sup>-1</sup> in 2007/2008; Nottingham  
 375 et al., 2010) close to our P8 and P19 sites (Figure S1). Finally, three of our sites (Met, P27 and  
 376 P19) were mature secondary forests, with tree densities (particularly at Met and P27; see 2.1)  
 377 lower than the old growth forests on BCI (Pyke et al., 2001) and Gigante (Koehler et al., 2009a).  
 378 This may have additionally influenced soil CO<sub>2</sub> fluxes since up to 35 % of CO<sub>2</sub> emissions can be  
 379 contributed by root respiration (Silver et al., 2005).

380 Soil CO<sub>2</sub> emissions responded to changes in climatic factors on a seasonal scale (i.e.  
 381 higher soil CO<sub>2</sub> fluxes in the wet than dry season at all sites; Table 3) and to daily fluctuations in  
 382 soil temperature and moisture across the five sites (see 3.2). The higher CO<sub>2</sub> emissions in the wet  
 383 season were likely due to the alleviation of water competition between decomposers and  
 384 vegetation; in seasonal tropical forests, litter tends to fall in the dry season, but low soil moisture  
 385 limits decomposition until the start of the wet season (Yavitt et al., 2004). Other studies from  
 386 CSA lowland forests have also reported a positive relationship between soil CO<sub>2</sub> emissions and  
 387 soil temperature (Chambers et al., 2004; Schwendenmann and Veldkamp, 2006; Sotta et al.,  
 388 2006, Koehler et al., 2009a), and parabolic relationships (Fig. 3) between soil CO<sub>2</sub> emissions and  
 389 soil moisture (Schwendenmann et al., 2003; Sotta et al., 2006; Kohler et al., 2009). Additionally,  
 390 soil CO<sub>2</sub> emissions responded to changes in soil mineral N both on the plot level and across sites  
 391 (see 3.2). Relationships between soil CO<sub>2</sub> emissions and soil mineral N concentrations have not  
 392 been reported in other studies, although Schwendenmann et al. (2003) observed that spatial  
 393 differences in soil total N were positively correlated with soil CO<sub>2</sub> fluxes, and Koehler et al.  
 394 (2009a) found that chronic N addition decreased soil CO<sub>2</sub> fluxes in a montane tropical forest  
 395 (although not in a lowland forest). However, the correlations between CO<sub>2</sub> emissions and both



396  $\text{NH}_4^+$  (positive correlation) and  $\text{NO}_3^-$  (negative correlation) may also simply be reflecting a co-  
397 correlation between extractable mineral N and soil moisture (see 3.2).

398 In support of our hypothesis, we observed that annual soil  $\text{CO}_2$  fluxes exhibited a  
399 parabolic pattern along the precipitation gradient (Table 4) similar to the relationship seen with  
400 the daily emissions and soil moisture (Fig. 3). However, soil  $\text{CO}_2$  efflux did not differ among the  
401 five forest sites of this precipitation gradient (Table 3). This lack of differences between sites  
402 could be due to similarity of a soil-controlling factor that results in comparably low soil  $\text{CO}_2$   
403 emissions at all sites. For example, although organic C and total N differed between sites, the  
404 soil C:N ratios were comparable along these orthogonal gradients of annual precipitation and soil  
405 fertility (Table 2), suggesting that the bioavailability of soil organic matter for heterotrophic  
406 respiration may be similar across sites. Additionally, the microbial communities that contribute  
407 to heterotrophic respiration may have adapted to the existing differences in substrate quantity  
408 (e.g. soil organic C), soil and climatic characteristics between the sites (Tables 2 and 3) and  
409 therefore exhibited an overall similar soil  $\text{CO}_2$  efflux.

410

#### 411 **4.2 $\text{CH}_4$ fluxes**

412 Our annual soil  $\text{CH}_4$  uptake (Table 4) was within the range of other reported values from Brazil  
413 and Panama (Verchot et al., 2000; Davidson et al., 2004; Keller et al., 2005; Silver et al., 2005;  
414 Veldkamp et al., 2013) although studies have also measured stronger uptake in CSA lowland  
415 forests (up to  $4.90 \text{ kg C ha}^{-1} \text{ yr}^{-1}$ ; Keller and Reiners, 1994; Steudler et al., 1996; Keller et al.,  
416 2005; Sousa Neto et al., 2011). Studies that measured higher uptake may have had soils with  
417 higher gas diffusivity due to lower soil water content and/or lower clay content (see Veldkamp et



al., 2013); in our five sites, the two sites with the highest sand content (P8 and P19; Table 1) exhibited the highest soil CH<sub>4</sub> uptake (Tables 3 and 4).

As shown in several CSA tropical forest studies (Keller and Reiners, 1994; Verchot et al., 2000; Davidson et al., 2004; Veldkamp et al., 2013), soil CH<sub>4</sub> fluxes are strongly regulated by soil moisture content. Soil CH<sub>4</sub> fluxes from our sites exhibited this expected pattern, with regards to less uptake during periods of high water content (i.e. wet vs. dry season; Table 3) as well as a positive correlation of soil CH<sub>4</sub> fluxes with water content (Fig. 4a). This we attributed to limited gas diffusivity from the atmosphere into the soil and/or methanogenic activity during periods of high moisture. Another soil factor controlling the temporal soil CH<sub>4</sub> uptake in our sites may have been soil NO<sub>3</sub><sup>-</sup>, as we observed increased CH<sub>4</sub> uptake as NO<sub>3</sub><sup>-</sup> concentrations increased in P8, P19 and P32 (see 3.3). Although this could be a co-correlation between soil NO<sub>3</sub><sup>-</sup> concentration and soil moisture (see 3.1), increasing CH<sub>4</sub> uptake in the soil with increasing mineral N has been observed in tropical forest soils of Australia (Kiese et al., 2003), Panama (Veldkamp et al., 2013) and Indonesia (Hassler et al., 2013). Additionally, our soils exhibited a correlation between annual soil CH<sub>4</sub> fluxes and soil <sup>15</sup>N natural abundance signatures (Table 5), the latter being an indicator of soil N availability (Sotta et al. 2008; Arnold et al. 2009; Baldos et al. 2015). When separated by season, the correlation between soil CH<sub>4</sub> fluxes and soil <sup>15</sup>N natural abundance was stronger in the dry season than the wet season (Table S1), supporting our claim that soil N availability enhanced CH<sub>4</sub> uptake in soils when gas diffusion was favorable (dry season).

The negative correlation between annual soil CH<sub>4</sub> uptake and annual precipitation (Fig. 4c; see 3.3) seemed at first to conflict with the mechanism we explained above for the positive correlation with soil moisture content (Fig. 4a). However, we attribute this to the fact that annual



precipitation was not the underlying factor controlling the annual soil CH<sub>4</sub> fluxes across these sites. Instead, the best indicator for annual soil CH<sub>4</sub> flux across the five sites was soil fertility (Fig. 4b), which showed an opposite pattern to that of annual precipitation (Figure S2). This soil fertility control was supported by the strong correlations of both annual (Table 5) and seasonal (Table S1) soil CH<sub>4</sub> fluxes with ECEC and exchangeable Al, both included in the soil fertility index (Figure S2; see 2.4). The negative correlation of soil CH<sub>4</sub> fluxes with exchangeable Al, which was clearly observed in the wet season (Table S1), could suggest an inhibition of methanogens by water-soluble Al (as opposed to inhibiting methanotrophs, as seen by Tamai et al., 2003). The correlations between soil CH<sub>4</sub> fluxes and fertility indicators reflected the site differences in soil biochemical characteristics (Table 2). Specifically, as shown by the strong inverse correlation between soil  $\delta^{15}\text{N}$  natural abundance signatures and exchangeable cations (Table 5), the positive correlation between soil CH<sub>4</sub> flux and fertility (Fig. 4b) likely reflected the long-term effects of soil development (Tables 1 and 2) - more CH<sub>4</sub> uptake occurred in highly weathered soils with less rock-derived nutrients but high soil N availability (i.e. high  $\delta^{15}\text{N}$  natural abundance signatures) (Tables 4 and 5). This supports our hypothesis that soil CH<sub>4</sub> uptake reflected the control of soil moisture and N availability across sites along this precipitation gradient. Our results also highlight the importance of considering soil properties - in particular the degree of soil development - rather than simply climatic factors, when predicting/modeling soil CH<sub>4</sub> fluxes on a large scale.

### 4.3 N<sub>2</sub>O fluxes

Our annual soil N<sub>2</sub>O fluxes (Table 4) were within the lower end of the range (1.23 - 11.4 kg N ha<sup>-1</sup> yr<sup>-1</sup>) reported from other CSA forest studies (Keller and Reiners 1994, Verchot et al., 1999,



464 Keller et al., 2005, Silver et al., 2005). In comparison with other studies from Panama, our N<sub>2</sub>O  
465 fluxes were similar to those measured from Gigante during dry years ( $0.5 \pm 0.2 \text{ kg N ha}^{-1} \text{ yr}^{-1}$  in  
466 2008–2009 with annual precipitation 5–26 % lower than the 12-year average; Corre et al. 2014)  
467 but slightly lower than those measured from the same site during wet years ( $1.0 - 1.4 \text{ kg N ha}^{-1}$   
468  $\text{yr}^{-1}$  in 2006–2007 with annual precipitation 5–17 % higher than the 12-year average; Koehler et  
469 al., 2009b). The low soil N<sub>2</sub>O fluxes at our sites were likely caused by the generally lower soil N  
470 availability compared to the Gigante site; the five sites in our present study had an average gross  
471 N mineralization rate of  $4 \pm 1 \text{ mg N kg}^{-1} \text{ d}^{-1}$  in the 2010 wet season (Corre et al. unpublished  
472 data), which was significantly lower than those from Gigante ( $29 \pm 6 \text{ mg N kg}^{-1} \text{ d}^{-1}$  in the 2006  
473 wet season; Corre et al. 2010). In addition, inter-annual variation in rainfall and hence soil  
474 moisture can strongly affect soil N<sub>2</sub>O emissions (Corre et al., 2014). Our measured soil N<sub>2</sub>O  
475 emissions exhibited a tendency to be higher in the wet season than the dry season (P8 and P19;  
476 Table 3), highest at the mid-rainfall site of P8 (which could mean that at the high-rainfall sites  
477 N<sub>2</sub>O could have been further denitrified to N<sub>2</sub>), and were only correlated with the soil <sup>15</sup>N natural  
478 abundance signatures (as an indicator of soil N availability) in the wet season (Table S1). At the  
479 sites (P8 and P19), where N<sub>2</sub>O emissions were higher in the wet than dry season and soil NO<sub>3</sub><sup>-</sup>  
480 levels were lower in the wet than dry season (Table 3), the inverse correlation between daily soil  
481 N<sub>2</sub>O emissions with NO<sub>3</sub><sup>-</sup> concentrations over the 21-month measurement period suggests that  
482 during the wet season N<sub>2</sub>O production could have been high but might have been further  
483 denitrified to N<sub>2</sub>, and hence resulted in low soil NO<sub>3</sub><sup>-</sup> concentrations. This argument is supported  
484 by our earlier study in Gigante, where nitrification and denitrification contributed equally to soil  
485 N<sub>2</sub>O emissions during the dry season but denitrification was the main process contributing to soil  
486 N<sub>2</sub>O emission in the wet season (Koehler et al., 2012; Corre et al. 2014). Our results partly



487 supported our hypothesis in that soil  $\text{N}_2\text{O}$  emissions were highest at the mid-precipitation site  
 488 (with the highest soil N availability as indicated by  $^{15}\text{N}$  natural abundance; Table 2) due to  
 489 possible reduction of  $\text{N}_2\text{O}$  to  $\text{N}_2$  at the high precipitation site.

490

#### 491 **4.4 NO fluxes**

492 Our annual soil NO uptake (Table 4) was considerably lower than other reported NO fluxes,  
 493 which are usually small net emissions rather than net uptake. Soil NO emissions from Panama,  
 494 Costa Rica and Brazil range from 0.26 to 7.88 kg N ha<sup>-1</sup>yr<sup>-1</sup> (Keller and Reiners 1994, Verchot et  
 495 al., 1999, Gut et al., 2002, Keller et al., 2005, Silver et al., 2005, Koehler et al., 2009b; Corre et  
 496 al. 2014). However, the net uptake that we measured may be reflecting unusually high ambient  
 497 air NO concentrations in our forest sites as compared to forests from other studies. Although all  
 498 of our sites were located in mature-secondary or old-growth forests, the forests were located  
 499 within the Panama Canal watershed, where there is heavy, year-round marine traffic (~13,000  
 500 cargo ships in 2011; Hricko, 2012). Furthermore, the highest levels of soil NO uptake that we  
 501 measured were in the Met site (Table 4); in addition to being in the vicinity of the Panama Canal,  
 502 the park is located within the city limits of Panama City, which has a population of  
 503 approximately 1.6 million people (The World Factbook, 2015). Therefore, elevated ambient air  
 504 NO concentrations from anthropogenic emissions may be driving the NO uptake that we  
 505 measured. Our instrument cannot measure  $\text{O}_3$  concentration, which could be high in these sites  
 506 influenced by anthropogenic emissions. Thus, the NO uptake that we saw may have been driven  
 507 by both chemical (Pape et al. 2009) and microbiological reactions (as NO is an intermediate  
 508 product of nitrification and denitrification; Davidson et al. 2000). The dominance of a chemical  
 509 reaction of NO uptake at our sites was supported by the fact that we observed a negative



510 correlation of soil NO fluxes with ambient air NO concentrations (i.e. net NO uptake increased  
511 as ambient air NO concentration increased; Fig. 5). The reaction of NO with O<sub>3</sub>, which is then  
512 subsequently removed from the enclosed chamber air and deposited onto the soil, is driven by  
513 the ambient air NO concentrations (Pape et al. 2009). This can occur in under a minute (which  
514 we observed on days with low ambient air NO concentrations when we measured net soil NO  
515 emissions; e.g. at P8 during the dry season, Fig. 2b) or can take up to the same order of  
516 magnitude as the turnover time of the chamber air (which we observed on days with high  
517 ambient air NO concentrations when we measured net NO uptake; e.g. at the Met site on most of  
518 the sampling days, Fig. 2b). It is notable, that an earlier study in Gigante, which is also part of  
519 the Panama Canal watershed, did not show net NO uptake but instead small net NO emissions  
520 (Koehler et al., 2009b; Corre et al. 2014). However, as mentioned above, the Gigante site had  
521 higher soil N-cycling rates (Corre et al. 2010) and lower ambient air NO concentrations than our  
522 sites, such that NO production in the soil overrides the chemical reaction of NO uptake and thus  
523 resulted in net soil NO emissions.

524       The general trend across sites did not support our hypothesis regarding soil NO emission,  
525 since local conditions of high ambient NO concentrations in the atmosphere had an overriding  
526 effect resulting in net NO uptake in soils (Fig. 2d). However, our results indicated that our soils  
527 could also be a net source of NO when soil conditions were favourable and/or ambient air NO  
528 concentrations were not elevated. We observed that net NO uptake was consistently higher in the  
529 wet season than the dry season (Table 3); in the dry season, when aerobic soil conditions  
530 prevailed due to low soil moisture contents (Table 3), NO production in the soil may have been  
531 more favoured (Conrad, 2002), partly counteracting the chemical reaction of NO removal from  
532 the atmosphere and its deposition onto the soil. This is also supported by the negative correlation





533 between dry-season soil NO fluxes and clay contents of the sites (Table S1), suggesting that soil  
534 NO fluxes were responding to conditions favourable for NO production. Favourable soil  
535 conditions were most visible at P8, which had the highest soil NO emissions (with low ambient  
536 air NO concentrations) in the dry season (Table 3; Fig. 2d); soil NO fluxes at this site increased  
537 when aerobic soil conditions prevailed (i.e. negative correlation with soil moisture; see 3.5) and  
538 increased with substrate availability (i.e. positive correlation with soil NO<sub>3</sub><sup>-</sup>; see 3.5).

539

#### 540 **4.5 Implications for climate change**

541 It is notable that, although all four trace gases were strongly correlated with the temporal  
542 variation in soil moisture and had clear differences between seasons (Table 3), there were no  
543 correlations between the soil trace gases when looking at the annual fluxes (Table 5) or seasonal  
544 averages (Table S1). This lack of correlation is presumably rooted in the interaction of other soil  
545 and/or climatic factors with known drivers of soil trace gas production and consumption. We  
546 have shown that in the short term, soil trace gas fluxes were largely controlled by soil moisture,  
547 with the additional influences of soil temperature and mineral N concentration. However, in the  
548 long term and/or over large spatial scales, the degree of soil development and related soil fertility  
549 had a strong influence. Additionally, we have shown that even in presently undisturbed forests,  
550 gas fluxes can be affected by ‘upstream’ anthropogenic activities. Therefore, in order to  
551 understand and be able to predict soil trace gas fluxes under future climate scenarios, research  
552 needs to focus on identifying and predicting interacting effects of soil and site, as well as  
553 climatic characteristics, on soil-atmosphere trace gas exchange.

554



## 555 **Acknowledgements**

556 Funding for this study was provided by the Deutsche Forschungsgemeinschaft (DFG, Co 749/1-  
 557 1) and by the Robert Bosch Foundation (Germany) for M.D. Corre's independent research group,  
 558 NITROF. We gratefully acknowledge Dr. Helene Muller-Landau for hosting us and facilitating  
 559 access to the field sites. The Smithsonian Tropical Research Institute and ANAM, Panama  
 560 provided invaluable administrative and technical support. The efforts of the NITROF assistants  
 561 (Rodolfo Rojas and Erick Diaz), and the SSTSE laboratory technicians in completing the data  
 562 collection and analyses were much appreciated.

563

## 564 **References**

- 565 Allen, K., Corre, M. D., Tjoa, A. and Veldkamp, E.: Soil nitrogen-cycling responses to  
 566 conversion of lowland forests to oil palm and rubber plantations in Sumatra, Indonesia,  
 567 PLoS ONE, 10(7), e0133325, doi:10.1371/journal.pone.0133325, 2015.
- 568 Bouwman, A. F., Fung, I., Matthews, E., and John, J.: Global analysis of the potential for N<sub>2</sub>O  
 569 production in natural soils. Global Biogeochem. Cy., 7, 557–597, 1993.
- 570 Butterbach-Bahl, K., Baggs, E. M., Dannenmann, M., Kiese, R., and Zechmeister-Boltenstern,  
 571 S.: Nitrous oxide emissions from soils: how well do we understand the processes and  
 572 their controls? Phil. Trans. R. Soc., 368, 20130122, 2013.
- 573 Chambers, J. Q., Tibuzy, E. S., Toledo, L. C., Crispim, B. F., Iguchi, N., dos Santos, J., Araujo,  
 574 A. C., Kruijt, B., Nobre, A. D., and Trumbore, S. E.: Respiration from a tropical forest  
 575 ecosystem: partitioning of sources and low carbon use efficiency. Ecol. Appl., 14, S72–  
 576 S88, 2004.



- 577 Chameides, W. L., Fehsenfeld, F., and Rodgers, M. O.: Ozone precursor relationships in the  
578 ambient atmosphere. *J. Geophys. Res.*, 97, 6037–6055, 1992.
- 579 Chin, K. J., Lukow, T., and Conrad, R.: Effect of temperature on structure and function of the  
580 methanogenic archaeal community in an anoxic rice field soil. *Appl. Environ. Microbiol.*,  
581 65, 2341–2349, 1999.
- 582 Conrad, R.: Soil microorganisms as controllers of atmospheric trace gases (H<sub>2</sub>, CO, CH<sub>4</sub>, OCS,  
583 N<sub>2</sub>O, and NO). *Microbiol. Rev.*, 60, 609–640, 1996.
- 584 Conrad, R.: Microbiological and biochemical background of production and consumption of NO  
585 and N<sub>2</sub>O in soil. In: *Trace Gas Exchange in Forest Ecosystems*, (eds Gasche R, Papen H,  
586 Rennenberg H), Dordrecht, Kluwer Academic Publishers, pp 3–33, 2002.
- 587 Corre, M. D., Veldkamp, E., Arnold, J., and Wright, S. J.: Impact of elevated N input on soil N  
588 cycling and losses in old-growth lowland and montane forests in Panama. *Ecology*, 91,  
589 1715–1729, 2010.
- 590 Corre, M. D., Sueta, J. P., and Veldkamp, E.: Nitrogen-oxide emissions from tropical forest soils  
591 exposed to elevated nitrogen input strongly interact with rainfall quantity and seasonality.  
592 *Biogeochemistry*, 118, 103–120, 2014.
- 593 Crawley, M. J.: *The R book*, Chichester: John Wiley, 2012.
- 594 Davidson, E. A., and Schimel, J. P.: Microbial processes of production and consumption of nitric  
595 oxide, nitrous oxide and methane. In: *Biogenic trace gases: measuring emissions from*  
596 *soil and water* (eds Matson PA, Harriss RC), Blackwell Science, Oxford, pp 327–357,  
597 1995.



- 598 Davidson, E. A., Verchot, L. V., Cattânio, J. H., Ackerman, I. L. and Carvalho, J. E. M.: Effects  
599 of soil water content on soil respiration in forests and cattle pastures of eastern Amazonia.  
600 Biogeochemistry, 48, 53–69, 2000.
- 601 Davidson, E. A., Yoko Ishida, F., and Nepstad, D. C.: Effects of an experimental drought on soil  
602 emissions of carbon dioxide, methane, nitrous oxide, and nitric oxide in a moist tropical  
603 forest. Glob. Change Biol., 10, 718–730, doi: 10.1111/j.1529-8817.2003.00762.x, 2004.
- 604 Gut, A., S. M. van Dijk, M. Scheibe, U. Rummel, M. Welling, C. Ammann, F. X. Meixner, G. A.  
605 Kirkman, M. O. Andreae, and B. E. Lehmann, NO emission from an Amazonian rain  
606 forest soil: Continuous measurements of NO flux and soil concentration, J. Geophys.  
607 Res., 107(D20), 8057, doi:10.1029/2001JD000521, 2002.
- 608 Hassler, E., Corre, M. D., Tjoa, A., Damris, M., Utami, S. R., and Veldkamp, E.: Soil fertility  
609 controls soil-atmosphere carbon dioxide and methane fluxes in a tropical landscape  
610 converted from lowland forest to rubber and oil palm plantations. Biogeosciences 12:  
611 5831–5852. DOI: 10.5194/bg-12-5831-2015, 2015.
- 612 Holtgrieve, G. W., Jewett, P. K. and Matson, P. A.: Variations in soil N cycling and trace gas  
613 emissions in wet tropical forests. Oecologia, 146, 584–594, 2006.
- 614 Hricko, A.: Progress and pollution: port cities prepare for the Panama Canal expansion.  
615 Environ. Health Persp., 120, A470–32012, 2012.
- 616 Jenny, H.: Arrangement of soil series and types according to functions of soil-forming factors.  
617 Soil Sci., 61, 375–392, 1946.
- 618 Keller, M., and Reiners, W. A.: Soil-atmosphere exchange of nitrous oxide, nitric oxide, and  
619 methane under secondary succession of pasture to forest in the Atlantic lowlands of Costa  
620 Rica. Global Biogeochem. Cy., 8, 399–409, 1994.



- 621 Keller, M., Jacob, D. J., Wofsy S. C., and Harriss, R. C.: Effects of tropical deforestation on  
622 global and regional atmospheric chemistry. *Climatic Change*, 19, 139–158, 1991.
- 623 Keller, M., Varner, R., Dias, J. D., Silva, H., Crill, P., de Oliveira, R. C., and Asner, G. P.: Soil–  
624 atmosphere exchange of nitrous oxide, nitric oxide, methane, and carbon dioxide in  
625 logged and undisturbed forest in the Tapajos national forest. Brazil, *Earth Interact.*, 9, 1–  
626 28, 2005.
- 627 Kiese, R., Hewett, B., Graham, A., and Butterbach-Bahl, K.: Seasonal variability of N<sub>2</sub>O and  
628 CH<sub>4</sub> uptake by tropical rainforest soils of Queensland, Australia. *Global Biogeochem.*  
629 *Cy.*, 25 17, 1043, doi:10.1029/2002GB002014, 2003.
- 630 Koehler, B., Corre, M. D., Veldkamp, E., and Sueta, J. P.: Chronic nitrogen addition causes a  
631 reduction in soil carbon dioxide efflux during the high stem-growth period in a tropical  
632 montane forest but no response from a tropical lowland forest on a decadal time scale.  
633 *Biogeosciences*, 6, 2973–2983, 2009a.
- 634 Koehler, B., Corre, M. D., Veldkamp, E., Wullaert, H., and Wright, S. J.: Immediate and long-  
635 term nitrogen oxide emissions from tropical forest soils exposed to elevated nitrogen  
636 input. *Glob. Change Biol.*, 15, 2049–2066, 2009b.
- 637 Koehler, B., Zehe, E., Corre, M. D., and Veldkamp, E. An inverse analysis reveals limitations of  
638 the soil- CO<sub>2</sub> profile method to calculate CO<sub>2</sub> production for well-structured soils.  
639 *Biogeosciences*, 7: 2311–2325, 2010.
- 640 Koehler, B., Corre, M. D., Steger, K., Well, R., Zehe, E., Sueta, J. P. and Veldkamp, E. An in-  
641 depth look into a tropical lowland forest soil: how 9-11 years experimental nitrogen  
642 addition affected the contents of N<sub>2</sub>O, CO<sub>2</sub> and CH<sub>4</sub> down to 2-m depth. *Biogeochemistry*  
643 111: 695-713. Erratum in 111: 715-717, 2012.



- 644 Kursar, T. A.: Evaluation of soil respiration and soil CO<sub>2</sub> concentration in a lowland moist forest  
645 in Panama. *Plant Soil*, 113, 21–29, 1989.
- 646 Le Mer, J., and Roger, P.: Production, oxidation, emission and consumption of methane by soils:  
647 a review. *Eur. J. Soil Biol.*, 37, 25–50, 2001.
- 648 Mariotti, A., Germon, J. C., Hubert, P., Kaiser, P., Letolle, R., Tardieux, A., and Tardieux, P.:  
649 Experimental determination of nitrogen kinetic isotope fractionation: some principles;  
650 illustration for the denitrification and nitrification processes. *Plant Soil*, 62, 413–430,  
651 1981.
- 652 Mohanty, S. R., Bodelier, P. L. E., and Conrad, R.: Effect of temperature on composition of the  
653 methanotrophic community in rice field and forest soil. *FEMS Microbiol. Ecol.*, 62, 24–  
654 31, 2007.
- 655 Nottingham, A. T., Turner, B. L., Winter, K., van der Heijden, M. G., and Tanner, E. V.:  
656 Arbuscular mycorrhizal mycelial respiration in a moist tropical forest. *New Phytol.*, 186,  
657 957–967, 2010.
- 658 Pape, L., Ammann, C., Nyfeler-Brunner, A., Spirig, C., Hens, K., and Meixner, F. X.: An  
659 automated dynamic chamber system for surface exchange measurement of non-reactive  
660 and reactive trace gases of grasslandecosystems. *Biogeosciences*, 6, 405–429, 2009.
- 661 Prather, M., Derwent, R., Ehhalt, D., Fraser, P., Sanhueza, E., and Zhou, X.: Other trace gases  
662 and atmospheric chemistry. In: *Climate Change 1994* (eds Houghton JT, Meira Filho LG,  
663 Bruce J, Lee H, Callander BA, Haites E, Harris N, Maskell K), Cambridge University  
664 Press, Cambridge, UK, 73–126, 1995.
- 665 Pyke, C. R., Condit, R., Aguilar, S., and Lao, S.: Floristic composition across a climatic gradient  
666 in a neotropical lowland forest. *J. Veg. Sci.*, 12, 553–566, 2001.



- 667 R Core Team. R: A language and environment for statistical computing. R Foundation for  
668 Statistical Computing, Vienna, Austria, ISBN 3-900051-07-0, URL: [http://www.R-](http://www.R-project.org/)  
669 [project.org/](http://www.R-project.org/), 2013.
- 670 Raich, J. W., and Schlesinger, W. H.: The global carbon dioxide flux in soil respiration and  
671 relationship to vegetation and climate. *Tellus*, 44B, 81–99, 1992.
- 672 Rummel, U., C. Ammann, A. Gut, F. X. Meixner, and M. O. Andreae, Eddy covariance  
673 measurements of nitric oxide flux within an Amazonian rain forest, *J. Geophys. Res.*,  
674 107(D20), 8050, doi:10.1029/2001JD000520, 2002
- 675 Saikawa, E., Schlosser, C. A., and Prinn, R. G.: Global modeling of soil nitrous oxide emissions  
676 from natural processes. *Global Biogeochem. Cy.*, 27, doi:10.1002/gbc.20087, 2013.
- 677 Santiago, L.S., Schuur, E.A. and Silvera, K.: Nutrient cycling and plant–soil feedbacks along a  
678 precipitation gradient in lowland Panama. *J. Trop. Ecol.*, 21, 461–470, 2005.
- 679 Schwendenmann, L., and Veldkamp, E.: Long-term CO<sub>2</sub> production from deeply weathered soils  
680 of a tropical rain forest: Evidence for a potential positive feedback to climate warming.  
681 *Glob. Change Biol.*, 12, 1878–1893, 2006.
- 682 Schwendenmann, L., Veldkamp, E., Brenes, T., O’Brien J. J., and Mackensen, J.: Spatial and  
683 temporal variation in soil CO<sub>2</sub> efflux in an old-growth neotropical rain forest, La Selva,  
684 Costa Rica. *Biogeochemistry*, 64, 111–128, 2003.
- 685 Silver, W.L., Neff, J., McGroddy, M., Veldkamp, E., Keller, M., and Cosme, R., Effects of Soil  
686 Texture on Belowground Carbon and Nutrient Storage in a Lowland Amazonian Forest  
687 Ecosystem. *Ecosystems*, 3, 193–209. doi:10.1007/s100210000019, 2000.



- 688 Silver, W. L., Thompson, A. W., McGroddy, M. E., Varner, R. K., Dias, J. D., Silva, H., Crill, P.  
689 M., and Keller, M.: Fine root dynamics and trace gas fluxes in two lowland tropical forest  
690 soils. *Glob. Change Biol.*, 11, 290–306, doi: 10.1111/j.1365-2486.2005.00903.x, 2005.
- 691 Sotta, E. D., Veldkamp, E., Guimaraes, B. R., Paixao, R. K., Ruivo, M. L. P., and Almeida, S. S.:  
692 Landscape and climatic controls on spatial and temporal variation in soil CO<sub>2</sub> efflux in an  
693 Eastern Amazonian Rainforest, Caxiuana, Brazil. *Forest Ecol. Manag.*, 237, 57–64, 2006.
- 694 Sotta, E. D., Corre, M. D., and Veldkamp, E.: Differing N status and N retention processes of  
695 soils under old-growth lowland forest in Eastern Amazonia, Caxiuanã, Brazil. *Soil Biol.*  
696 *Biochem.*, 40, 740–750, 2008.
- 697 Sousa Neto, E., Carmo, J. B., Keller, M., Martins, S. C., Alves, L. F., Vieira, S. A., Piccolo, M.  
698 C., Camargo, P., Couto, H. T. Z., Joly, C. A., and Martinelli, L. A.: Soil-atmosphere  
699 exchange of nitrous oxide, methane and carbon dioxide in a gradient of elevation in the  
700 coastal Brazilian Atlantic forest. *Biogeosciences*, 8, 733–742, doi:10.5194/bg-8-733-  
701 2011, 2011.
- 702 Steudler, P. A., Melillo, J. M., Feigl, B. J., Neill, C., Piccolo, M. C., and Cerri, C. C.:  
703 Consequences of forest-to-pasture conversion on CH<sub>4</sub> fluxes in the Brazilian Amazon  
704 Basin. *J. Geophys. Res.-Atmos.*, 101, 18547–18554, doi:10.1029/96JD01551, 1996.
- 705 Stocker, T. F., Qin, D., Plattner, G. K., Tignor, M., Allen, S. K., Boschung, J., Nauels, A., Xia,  
706 Y., Bex, B., and Midgley, B. M.: IPCC, 2013: climate change 2013: the physical science  
707 basis. Contribution of working group I to the fifth assessment report of the  
708 intergovernmental panel on climate change. 2013.
- 709 Swaine MD. Rainfall and soil fertility as factors limiting forest species distributions in Ghana. *J.*  
710 *Ecol.*, 84, 419–428, 1996.





- 711 Tamai, N., Takenaka, C., Ishizuka, S., and Tezuka, T.: Methane flux and regulatory variables in  
712 soils of three equal-aged Japanese cypress (*Chamaecyparis obtusa*) forests in central  
713 Japan. *Soil Biol. Biochem.*, 35, 633–641, 2003.
- 714 The World Factbook. <https://www.cia.gov/library/publications/the-world-factbook/geos/pm.html>  
715 [Accessed: March, 2015]
- 716 Townsend, A. R., Asner, G. P., and Cleveland, C. C.: The biogeochemical heterogeneity of  
717 tropical forests. *Trends Ecol. Evol.*, 23, 424–431, 2008.
- 718 Turner, B. L., and Engelbrecht, B. M. J.: Soil organic phosphorus in lowland tropical rain forests.  
719 *Biogeochemistry*, 103, 295–315, 2011.
- 720 Veldkamp, E., B. Koehler, and M. D. Corre.: Indications of nitrogen-limited methane uptake in  
721 tropical forest soils. *Biogeosciences* 10, 5367–5379, 2013.
- 722 Verchot, L. V., Davidson, E. A., Cattânio, H., Ackerman, I. L., Erickson, H. E., and Keller, M.:  
723 Land use change and biogeochemical controls of nitrogen oxide emissions from soils in  
724 eastern Amazonia. *Global Biogeochem. Cy.*, 13(1), 31–46, 1999.
- 725 Verchot, L. V., Davidson, E. A., Cattânio, J. H., and Ackerman, I. L.: Land-use change and  
726 biogeochemical controls of methane fluxes in soils of eastern Amazonia. *Ecosystems*, 3,  
727 41–56, doi:10.1007/s100210000009, 2000.
- 728 Windsor, D. M.: Climate and moisture availability in a tropical forest, long term record for Barro  
729 Colorado Island, Panama. *Smithson. Contrib. Earth Sci.*, 29, 1–145, 1990.
- 730 Wright, S. J., Yavitt, J. B., Wurzbarger, N., Turner, B. L., Tanner, E. V., Sayer, E. J., Santiago,  
731 L. S., Kaspari, M., Hedin, L. O., Harms, K. E., Garcia, M. N., and Corre, M. D.  
732 Potassium, phosphorus, or nitrogen limit root allocation, tree growth, or litter production  
733 in a lowland tropical forest. *Ecology*, 92, 1616–1625, 2011.



- 734 Yavitt, J. B., Wright, S. J., and Kelman Wieder, R.: Seasonal drought and dry-season irrigation  
735 influence leaf-litter nutrients and soil enzymes in a moist, lowland forest in Panama.  
736 Austral Ecol., 29, 177–188, 2004.
- 737 Zuur, A.F., Ieno, E.N., Walker, N.J., Saveliev, A.A., and Smith, G.M.: Mixed effects models and  
738 extensions in ecology with R. Springer, New York., 2009.



739 **Table 1** Description of location, rainfall and geology of one hectare forest inventory plots located in the Panama Canal watershed,  
740 central Panama.

Plot code <sup>a</sup>	Longitude, latitude	Elevation (m above sea level)	Forest age classification <sup>a</sup>	Soil taxonomic order <sup>b</sup>	Soil texture (% sand/ silt/clay) <sup>c</sup>	Precipitation (mm yr <sup>-1</sup> ) <sup>b</sup>	Geology <sup>b</sup>
Metropolitan	79° 33' W, 8° 59' N	30	mature secondary	Inceptisol (Cambisol)	3/35/62	1700	Aglomerate of andesitic tuff, Early-Late Oligocene
P27	79° 38' W, 9° 4' N	160	mature secondary	Inceptisol (Cambisol)	2/38/60	2030	Aglomerate of siltstone, tuff and limestone, Early Miocene
P8	79° 44' W, 9° 10' N	50	old growth	Oxisol (Ferralsol)	12/39/48	2360	Basaltic and andesitic lavas and tuff, pre-Tertiary
P19	79° 46' W, 9° 11' N	160	mature secondary	Oxisol (Ferralsol)	10/27/63	2690	Basaltic and andesitic lavas and tuff, pre-Tertiary
P32	79° 43' W, 9° 21' N	340	old growth	Oxisol (Ferralsol)	1/39/60	3400	Basaltic and andesitic lavas and tuff, pre-Tertiary

741 <sup>a</sup> Plot codes and forest age classification are from Pyke et al. (2001).



742 <sup>b</sup> Turner and Engelbrecht (2011) reported the tentative soil order (based on US Soil Taxonomy with equivalent FAO classification in  
743 brackets), mean annual precipitation (estimated from location and elevation data as described by Engelbrecht et al. 2007), and the  
744 geological information (taken from Stewart et al. 1980).  
745 <sup>c</sup>Textural analyses are the weighted average of the sampling depth intervals: 0-5, 5-10, 10-25 and 25-50 cm.



**Table 2** Soil biochemical characteristics in the top 50 cm of lowland forest soils along orthogonal gradients of annual precipitation (shown in brackets below each site) and soil fertility in the Panama Canal watershed, central Panama.

Soil characteristics <sup>a</sup>	Metropolitan (1700 mm)	P27 (2030 mm)	P8 (2360 mm)	P19 (2690 mm)	P32 (3400 mm)
$\delta^{15}\text{N}$ enrichment factor, $\epsilon$ <sup>b</sup>	$-1.95 \pm 0.52$ <sup>b</sup>	$-0.37 \pm 1.69$ <sup>b</sup>	$-2.76 \pm 0.54$ <sup>ab</sup>	$-4.70 \pm 0.44$ <sup>a</sup>	$-2.65 \pm 0.30$ <sup>ab</sup>
$\delta^{15}\text{N}$ natural abundance (‰)	$5.9 \pm 0.8$ <sup>c</sup>	$6.3 \pm 0.4$ <sup>bc</sup>	$12.0 \pm 1.0$ <sup>a</sup>	$9.2 \pm 0.9$ <sup>a</sup>	$7.0 \pm 0.3$ <sup>b</sup>
Organic C (mg C g <sup>-1</sup> )	$12.8 \pm 1.7$ <sup>ab</sup>	$10.8 \pm 3.3$ <sup>b</sup>	$15.1 \pm 0.2$ <sup>ab</sup>	$15.0 \pm 1.3$ <sup>ab</sup>	$19.6 \pm 2.1$ <sup>a</sup>
Total N (mg C g <sup>-1</sup> )	$1.08 \pm 0.15$ <sup>b</sup>	$1.05 \pm 0.25$ <sup>b</sup>	$1.49 \pm 0.02$ <sup>ab</sup>	$1.44 \pm 0.11$ <sup>ab</sup>	$1.85 \pm 0.17$ <sup>a</sup>
C:N ratio	$10.9 \pm 4.1$ <sup>a</sup>	$9.07 \pm 1.8$ <sup>a</sup>	$9.76 \pm 1.0$ <sup>a</sup>	$9.88 \pm 1.0$ <sup>a</sup>	$10.1 \pm 1.2$ <sup>a</sup>
pH (1:4 H <sub>2</sub> O)	$6.20 \pm 0.46$ <sup>a</sup>	$5.82 \pm 0.72$ <sup>a</sup>	$5.05 \pm 0.17$ <sup>b</sup>	$4.88 \pm 0.30$ <sup>b</sup>	$5.14 \pm 0.22$ <sup>b</sup>
ECEC <sup>c</sup> (mmol <sub>c</sub> kg <sup>-1</sup> )	$199 \pm 72$ <sup>ab</sup>	$267 \pm 11$ <sup>a</sup>	$56 \pm 2$ <sup>c</sup>	$51 \pm 6$ <sup>c</sup>	$118 \pm 12$ <sup>bc</sup>
Exch. bases <sup>c</sup> (mmol <sub>c</sub> kg <sup>-1</sup> )	$198 \pm 72$ <sup>a</sup>	$264 \pm 10$ <sup>a</sup>	$37 \pm 6$ <sup>c</sup>	$21 \pm 8$ <sup>c</sup>	$90 \pm 11$ <sup>b</sup>
Exchangeable Al (mmol <sub>c</sub> kg <sup>-1</sup> )	$0.22 \pm 0.13$ <sup>b</sup>	$1.96 \pm 0.51$ <sup>b</sup>	$12.2 \pm 4.7$ <sup>ab</sup>	$22.6 \pm 7.3$ <sup>a</sup>	$22.2 \pm 3.2$ <sup>a</sup>

<sup>a</sup> Means ( $\pm$ SE,  $n = 4$ ) followed by different letters indicate significant differences between sites (one-way ANOVA with Tukey HSD at  $P \leq 0.05$ ). Values for each replicate plot are weighted average of the sampling depth intervals of 0-5, 5-10, 10-25 and 25-50 cm.

<sup>b</sup> Calculated using Rayleigh equation (Mariotti et al. 1981):  $\epsilon = d_s - d_{so} / \ln f$ ;  $d_s$ -  $\delta^{15}\text{N}$  natural abundance signatures at various depths in the soil profile,  $d_{so}$ -  $\delta^{15}\text{N}$  natural abundance of the reference depth (top 5cm) and  $f$  is the remaining fraction of total N (i.e. total N concentration at a given depth divided by the total N concentration in the top 5 cm).

<sup>c</sup> ECEC – Effective cation exchange capacity; Exch. bases – sum of exchangeable Ca, Mg, K, Na



**Table 3** Soil factors (measured in the top 5 cm of soil) and trace gas fluxes from lowland forest soils along orthogonal gradients of annual precipitation (mm per year; shown in brackets below each site) and soil fertility in the Panama Canal watershed, central Panama.

Site / season <sup>a</sup>	Soil temperature (°C)	Soil moisture (g g <sup>-1</sup> )	Soil NH <sub>4</sub> <sup>+</sup> (mg N kg <sup>-1</sup> )	Soil NO <sub>3</sub> <sup>-</sup> (mg N kg <sup>-1</sup> )	CO <sub>2</sub> flux (mg C m <sup>-2</sup> h <sup>-1</sup> )	CH <sub>4</sub> flux (μg C m <sup>-2</sup> h <sup>-1</sup> )	N <sub>2</sub> O flux (μg N m <sup>-2</sup> h <sup>-1</sup> )	NO flux (μg N m <sup>-2</sup> h <sup>-1</sup> )
<i>Wet season</i>								
Metropolitan (1700)	25.8 (0.4) <sup>a</sup>	0.64 (0.04) <sup>Ac</sup>	5.94 (1.52) <sup>b</sup>	1.95 (0.71) <sup>Ba</sup>	126 (26) <sup>A</sup>	1.47 (3.66) <sup>Aa</sup>	5.78 (2.69) <sup>b</sup>	-11.6 (7.08) <sup>Bb</sup>
P27 (2030)	25.2 (0.4) <sup>b</sup>	0.72 (0.06) <sup>Ab</sup>	6.39 (1.35) <sup>Aab</sup>	0.51 (0.17) <sup>Bc</sup>	124 (18) <sup>A</sup>	-3.01 (4.20) <sup>Aa</sup>	4.15 (2.56) <sup>b</sup>	-3.24 (2.68) <sup>Ba</sup>
P8 (2360)	25.6 (0.4) <sup>Aab</sup>	0.60 (0.03) <sup>Ac</sup>	5.68 (0.94) <sup>ab</sup>	1.32 (0.54) <sup>Bb</sup>	131 (19) <sup>A</sup>	-7.87 (6.95) <sup>Abc</sup>	13.5 (7.0) <sup>Aa</sup>	-3.95 (6.60) <sup>Ba</sup>
P19 (2690)	25.5 (0.5) <sup>ab</sup>	0.72 (0.06) <sup>Ab</sup>	7.29 (1.39) <sup>ab</sup>	0.46 (0.39) <sup>c</sup>	129 (15) <sup>A</sup>	-13.0 (6.92) <sup>Ac</sup>	5.58 (3.13) <sup>Ab</sup>	-3.98 (4.95) <sup>a</sup>
P32 (3400)	24.6 (0.4) <sup>c</sup>	0.90 (0.08) <sup>Aa</sup>	8.21 (1.87) <sup>Aa</sup>	0.49 (0.27) <sup>Bc</sup>	107 (17) <sup>A</sup>	-6.79 (6.09) <sup>Aab</sup>	6.41 (3.09) <sup>b</sup>	-4.01 (4.34) <sup>Ba</sup>
<i>Dry season</i>								
Metropolitan (1700)	25.3 (0.3) <sup>a</sup>	0.45 (0.06) <sup>Bb</sup>	5.32 (1.26) <sup>bc</sup>	3.42 (1.55) <sup>Aa</sup>	82.7 (19) <sup>B</sup>	-6.88 (4.14) <sup>Ba</sup>	4.18 (4.62)	-4.05 (7.21) <sup>Aab</sup>



P27 (2030)	24.7 (0.2) <sup>bc</sup>	0.53 (0.08) <sup>Bab</sup>	4.46 (0.89) <sup>Bc</sup>	0.79 (0.18) <sup>Ab</sup>	87.7 (14) <sup>B</sup>	-12.1 (3.1) <sup>Bab</sup>	4.87 (4.70)	1.09 (1.23) <sup>Aab</sup>
P8 (2360)	24.9 (0.3) <sup>Bab</sup>	0.48 (0.06) <sup>Bb</sup>	6.04 (1.15) <sup>abc</sup>	3.68 (1.16) <sup>Aa</sup>	85.7 (17) <sup>B</sup>	-21.3 (8.37) <sup>Bbc</sup>	5.64 (5.75) <sup>B</sup>	6.50 (3.76) <sup>Aa</sup>
P19 (2690)	25.0 (0.3) <sup>ab</sup>	0.49 (0.04) <sup>Bb</sup>	7.47 (1.22) <sup>ab</sup>	0.64 (0.26) <sup>b</sup>	85.5 (12) <sup>B</sup>	-29.2 (4.08) <sup>Bc</sup>	1.30 (3.09) <sup>B</sup>	-2.41 (2.35) <sup>b</sup>
P32 (3400)	24.4 (0.3) <sup>c</sup>	0.64 (0.09) <sup>Ba</sup>	7.86 (1.37) <sup>a</sup>	1.17 (0.61) <sup>Ab</sup>	78.5 (15) <sup>B</sup>	-17.4 (5.09) <sup>Bab</sup>	5.89 (5.51)	4.34 (2.23) <sup>Aa</sup>

<sup>a</sup> Means (( $\pm$ SE,  $n = 4$ ) followed by different lowercase letters indicate significant differences among sites within each season and

different uppercase letters indicate significant differences between seasons within each site (linear mixed effects model with Tukey

HSD test at  $P \leq 0.05$ ).



**Table 4** Annual<sup>a</sup> trace gas fluxes (mean (SE), n = 4) from lowland tropical forest soils along orthogonal gradients of annual precipitation and soil fertility in the Panama Canal watershed, central Panama.

Site (annual precipitation)	CO <sub>2</sub>	CH <sub>4</sub>	N <sub>2</sub> O	NO
	(Mg C ha <sup>-1</sup> yr <sup>-1</sup> )	(kg C ha <sup>-1</sup> yr <sup>-1</sup> )	(kg N ha <sup>-1</sup> yr <sup>-1</sup> )	(kg N ha <sup>-1</sup> yr <sup>-1</sup> )
Met (1700 mm)	8.48 (0.70)	-0.34 (0.17)	0.41 (0.06)	-0.82 (0.16)
P27 (2030 mm)	9.16 (0.62)	-0.51 (0.04)	0.43 (0.06)	-0.12 (0.04)
P8 (2360 mm)	10.14 (0.76)	-1.45 (0.15)	1.07 (0.15)	-0.17 (0.17)
P19 (2690 mm)	9.89 (0.49)	-1.98 (0.07)	0.35 (0.05)	-0.21 (0.10)
P32 (3400 mm)	7.89 (0.84)	-0.94 (0.19)	0.66 (0.18)	-0.03 (0.09)

<sup>a</sup> Calculated using the trapezoidal rule between fluxes and time interval, covering the measurement periods of January - December 2011 for CO<sub>2</sub>, CH<sub>4</sub> and N<sub>2</sub>O, and June 2010 - May 2011 for NO. Annual fluxes were not tested statically for differences among sites since these are trapezoidal extrapolations.





**Table 5** Spearman correlations of soil biochemical characteristics<sup>a</sup> and annual (measured in 2011) soil trace gas fluxes from five lowland tropical forests along orthogonal precipitation and fertility gradients in the Panama Canal watershed, central Panama.

	ECEC	BS	Na	Al	pH	Clay	CO <sub>2</sub>	CH <sub>4</sub>	N <sub>2</sub> O	NO
<sup>15</sup> N sig.	-0.87**	-0.67**	-0.30	0.42	-0.61**	-0.15	0.41	-0.70**	0.30	0.16
ECEC		0.80**	0.34	-0.50	0.76**	-0.12	-0.33	0.77**	-0.09	-0.17
BS			-0.13	-0.87**	0.96**	-0.12	-0.40	0.78**	-0.12	-0.54
Na				0.45	-0.18	-0.15	0.04	0.01	-0.01	0.60**
Al					-0.87**	0.04	0.24	-0.71**	0.17	0.58**
pH						-0.04	-0.34	0.76**	-0.12	-0.54
Clay							-0.13	-0.17	-0.67**	-0.34
CO <sub>2</sub>								-0.24	0.26	0.10
CH <sub>4</sub>									-0.07	-0.31
N <sub>2</sub> O										0.19

\*\*  $P < 0.01$ ,  $n = 20$  (4 replicate plots in each of the 5 forest sites)

<sup>a</sup> Soil parameter abbreviations: <sup>15</sup>N natural abundance signature (<sup>15</sup>N sig.), effective cation exchange capacity (ECEC) and base saturation (BS).

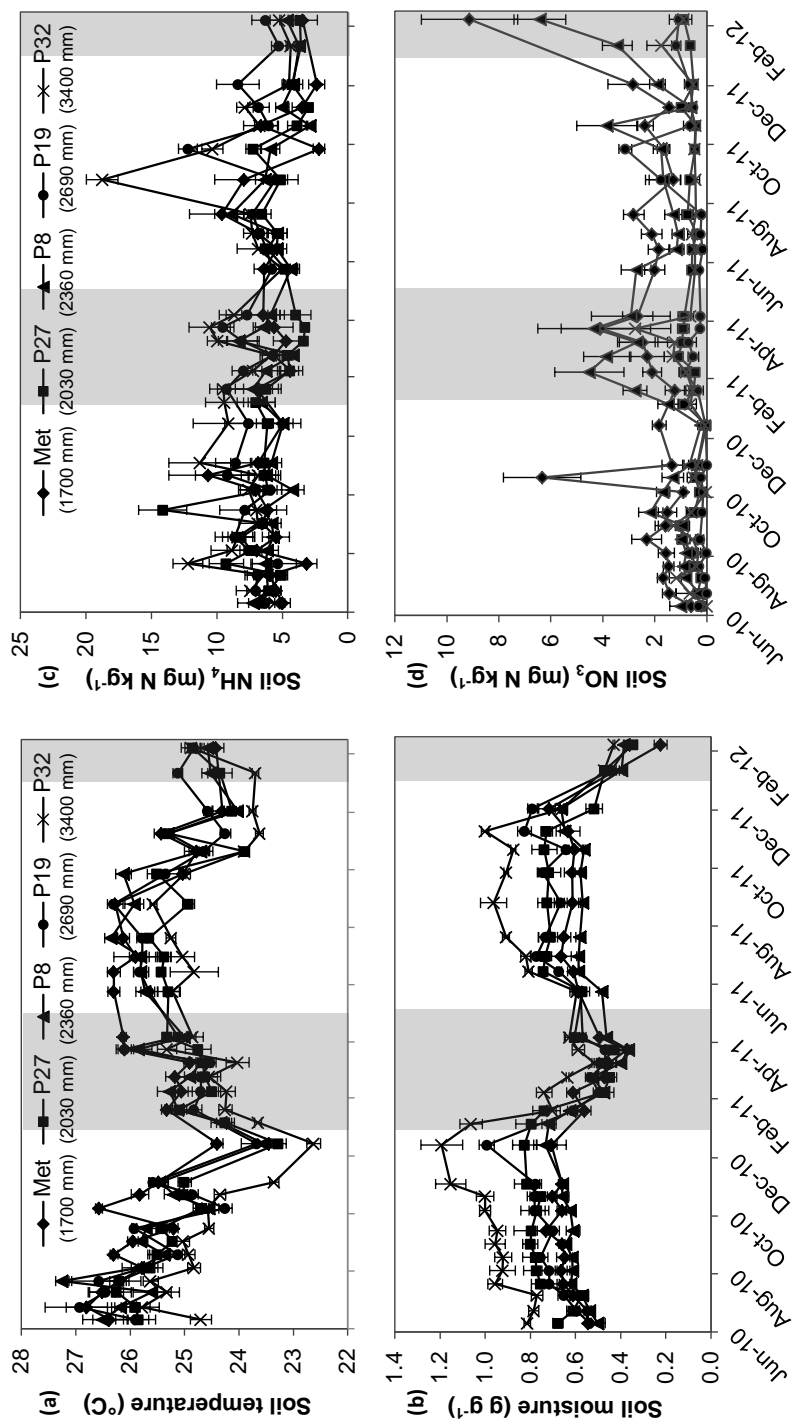


**Fig. 1** Mean ( $\pm$ SE,  $n = 4$ ) soil (a) temperature, (b) moisture, (c)  $\text{NH}_4^+$  and (d)  $\text{NO}_3^-$  concentrations measured in the top 5 cm of soil in lowland forests along orthogonal gradients of annual precipitation and soil fertility in the Panama Canal watershed, central Panama. Gray shading indicates the dry season (January through April).

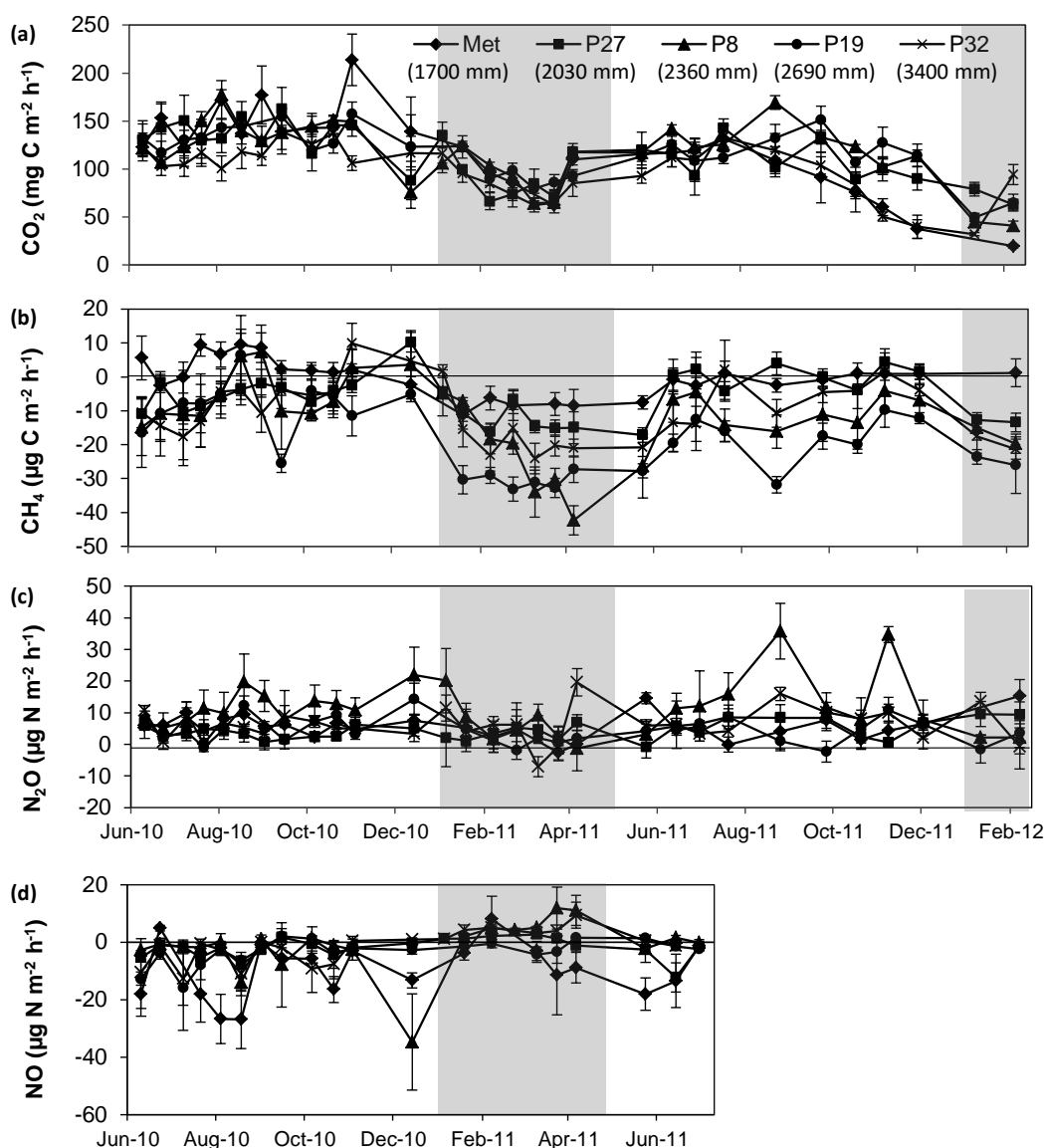
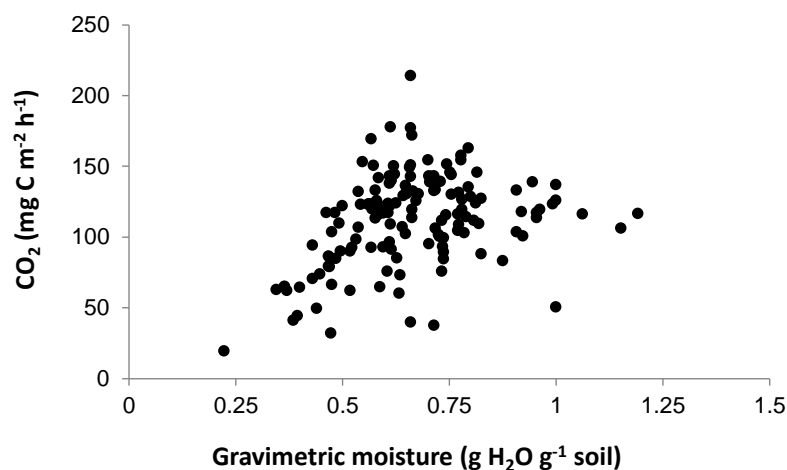


**Fig. 2** Mean ( $\pm$ SE,  $n = 4$ ) soil (a) CO<sub>2</sub>, (b) CH<sub>4</sub>, (c) N<sub>2</sub>O and (d) NO fluxes from lowland forests along orthogonal gradients of annual precipitation and soil fertility in the Panama Canal watershed, central Panama. Gray shading indicates the dry season (January through April).



32

33 **Fig. 3** Soil CO<sub>2</sub> fluxes and moisture contents (top 5 cm) in five lowland forests along orthogonal  
 34 gradients of annual precipitation and soil fertility in the Panama Canal watershed, central  
 35 Panama. Each data point is the average of four replicate plots on one sampling day from one of  
 36 the five sites, measured from June 2010 to February 2012 ( $n = 145$ ).

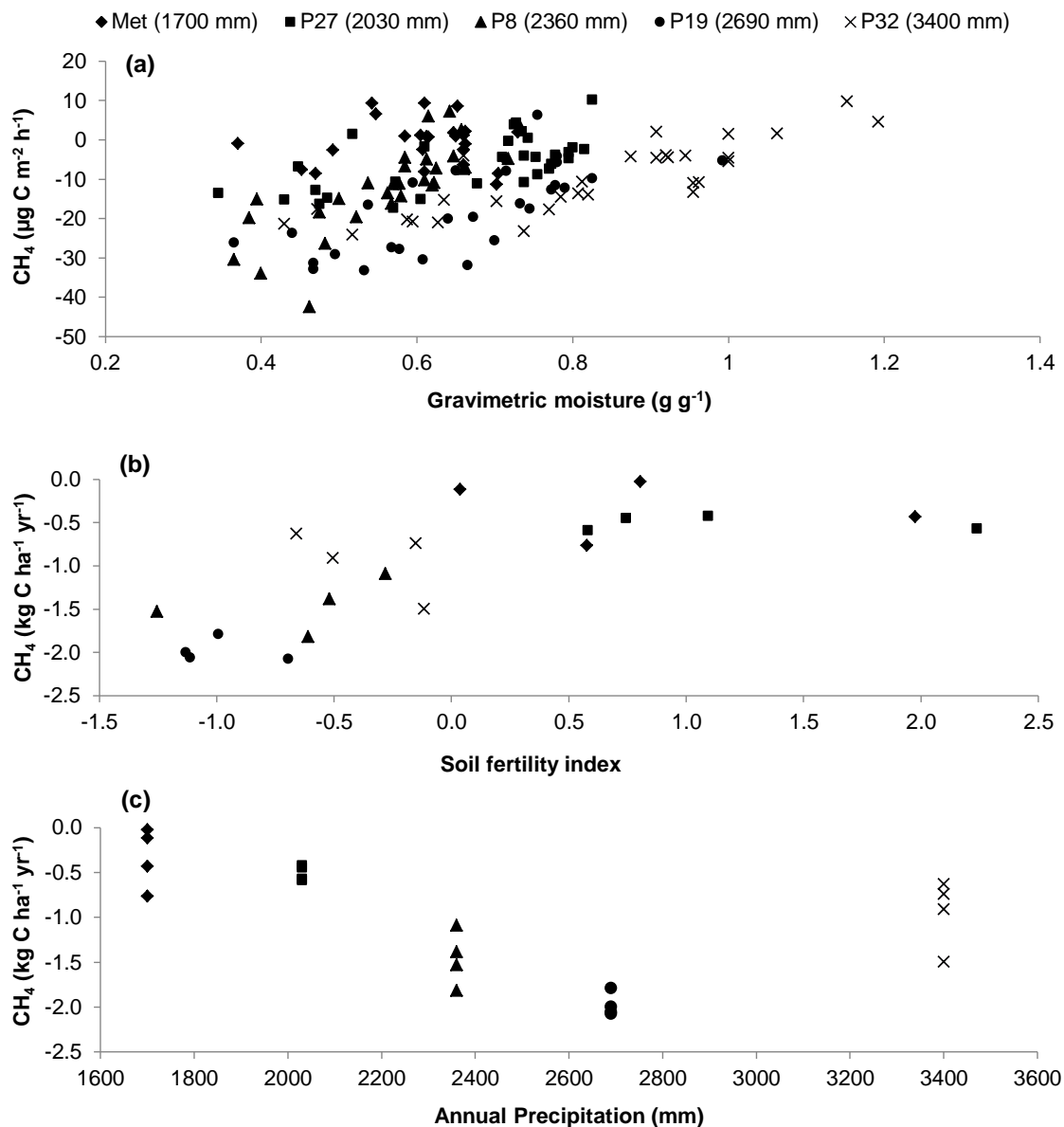
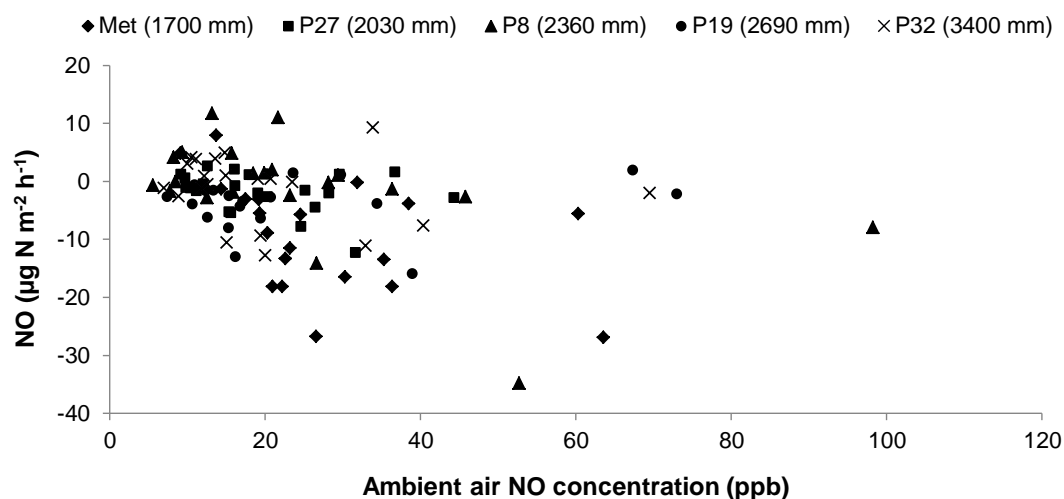


Fig. 4 Average daily soil CH<sub>4</sub> fluxes plotted against (a) soil moisture (top 5 cm), and annual soil CH<sub>4</sub> fluxes plotted against (b) soil fertility index and (c) annual precipitation. For (a), each data point is the average of four replicate plots on each sampling day of each of the five sites, measured from June 2010 to February 2012. The five lowland forests are located along orthogonal gradients of annual precipitation and soil fertility in the Panama Canal watershed, central Panama.



45



46

**Fig. 5** Soil NO fluxes plotted against ambient air NO concentrations; each data point is the average of four replicate plots on each sampling day in each of the five sites, measured from June 2010 to June 2011. The five lowland forests are located along orthogonal gradients of annual precipitation and soil fertility in the Panama Canal watershed, central Panama.